Supplementary Methods

Expression and immobilization of Methuselah ectodomain

A hexahistidine-tagged Mth ectodomain construct[1] was appended with a C-terminal biotinylation tag[2] and subcloned into the baculovirus transfer vector pVL1392. Mth was purified from supernatants of baculovirus-infected High 5 cells as described previously[1]. Purified Mth ectodomain was biotinylated *in vitro* with BirA, desalted, and immobilized on NeutrAvidin-Agarose (Pierce) to ~1 mg Mth per ml matrix.

In vitro *binding assays of mRNA display libraries*

^{35}S-methionine-labeled RNA-peptide fusions from each round of selection were purified, treated with RNase, and assayed for binding to Mth-agarose as described previously[3]. Individual peptides were also tested in this format by PCR amplification of specific clones with oligos 47T7FP and 21.2. Competition studies were performed by introducing various concentrations of unlabeled peptides into the binding buffer during the initial binding step.

Peptide synthesis

Peptides were synthesized, purified, and quantitated as described previously[3]. Several peptides were synthesized with an N-terminal spacer [8-(Fmoc-amino)-3,6-dioxa-octanoic acid, Bachem #B-3635] for conjugation to various functional groups (e.g., biotin, fluorescein, or rhodamine). Peptides sequences are shown in Table 1. The sequence of the scrambled version of R8-12 peptide is MLRARRHGVWSPLRFRIMV. The sequence of the EL2 peptide, derived from the 2nd extracellular loop of Mth, is

DNIVENQDWNPRVGHEGH. The R8-14 W7A peptide included a C-terminal Gly-Tyr for quantitation by spectrophotometry.

Spectrofluorometric analysis of Mth:peptide complexes

Measurements of intrinsic tryptophan and tyrosine fluorescence spectra were performed on a spectrofluorophotometer (RF-5301PC, Shimadzu Scientific Instruments) at excitation wavelengths of 280 or 295 nm (slit width set at 3 nm). Spectra were taken at room temperature from 260 to 450 nm at 0.2 nm intervals (medium speed, 3 or 5 nm slit widths for R8-12 or R8-04 peptides, respectively). Complexes were formed by mixing equimolar concentrations of peptide and Mth ectodomain in buffer (10 mM KH_2PO_4 at pH 7.2 and 150 mM NaCl) for 5 min before taking fluorescence readings in a stirred cell. For R8-04, 3 μM peptide and wild-type Mth ectodomain were used. The mutant ectodomain, Mth W120S, was used for complexes with R8-12 (both at 6.25 μM concentrations) because the peptide contains a single Trp residue. For the fluorescence titration study, 300 nM of R8-12 peptide was used and aliquots of Mth W120S were directly added to the stirring cell (excitation and emission wavelengths were set at 295 and 345 nm, with slit widths at 5 and 10 nm, respectively).

Crystallography – data collection, structure solution, and refinement

Purified His_6-tagged Mth ectodomain (15 mg ml^{-1}) was mixed with 1.5-fold molar excess R8-01 15-mer peptide in 10 mM Tris at pH 8.0. Crystals of the Mth:R8-01 complex were grown by hanging drop, in which the protein mixture was mixed 1:1 with well solution [0.1 M HEPES-KOH at pH 7.5, 1.7 M ammonium sulfate, and 2% (w/v) PEG 400]. The resulting 2 μl drop was suspended over 0.8 ml of well solution. Crystals were grown for

several months at room temperature and formed long rods with maximum dimensions of 200 μm × 50 μm × 50 μm.

Crystals were transferred to a cryoprotectant solution [(0.1 M HEPES-KOH at pH 7.5, 1.8 M ammonium sulfate, 2% PEG 400, and 20% (v/v) glycerol] prior to flash cooling. Data were collected at −150 °C at the Advanced Light Source beamline 9.2.2 with λ = 1.0781 Å (**Supp. Table 2**). Data were processed and scaled with DENZO and SCALEPACK[4]. The diffraction was strongly anisotropic, extending to ~2.5 Å along the 4-fold axis but only to ~3.8 Å perpendicular to the 4-fold with strong streaking in these directions. The crystals were initially indexed in space group $P4_2$, with a = 94.25 Å and c = 173.84 Å. R_{merge} from 20–3.50 Å (3.62–3.50 Å) was 15.5% (37.0%).

The structure was determined by molecular replacement using AMoRe[5] from version 5 of the CCP4 suite[6] with the 2.3 Å structure of the Mth ectodomain (PDB code 1FJR) as a search model. Examination of the native Patterson map revealed three very strong non-origin peaks implying translational non-crystallographic symmetry (NCS). A translational NCS vector was used during the translation function search. Two molecules were placed in the asymmetric unit in space group $P4_22_12$, which explained two of the three peaks in the native Patterson. Addition of a third molecule, necessary to give the third native Patterson peak, always resulted in steric clashes. The data was eventually explained by an extensive form of stacking disorder in the crystals, which was consistent with the observed symmetry of the Mth packing. Specifically, each stack of Mth 222 tetramers along the c axis can be at one of three heights, and the relative heights of adjacent stacks are partially random. This disorder is the likely cause of the strong anisotropy of the data and of the streaking of the diffraction spots. This stacking disorder

means that there is no true repeating unit cell for this crystal. Nevertheless, we modeled the disorder in $P4_2$ with one Mth molecule with unit occupancy and two with half occupancy. Maps were calculated with solvent flattening, histogram matching, and NCS averaging using the program DM in the CCP4 suite[6]. The Ramachandran statistics (PROCHECK) for the final structure were: most favored, 77.5%; additional allowed, 21.3 %; generously allowed, 1.2 %; disallowed, 0%. Anisotropy and bulk solvent corrections were applied and the model was refined with NCS constraints using grouped temperature (*B*) factors using the program CNS[7]. The peptide has been left unmodeled. The current model has R_{cryst} = 37.5% and R_{free} = 40.8%.

Fluorescence labeling of cells expressing Methuselah

Chinese hamster ovary (CHO) cells were transiently transfected with a Mth-GFP fusion construct and grown in alpha-MEM with 5% fetal bovine serum (FBS). Cells were detached by trypsination and washed with P4F (1× PBS with 4% FBS). Cells were then incubated with 150 nM rhodamine-R8-12 peptide in P4F for 1 h at 4 °C, washed extensively with P4F, and either mounted on glass slides for fluorescence microscopy or sorted by FACS (BD FACSCalibur System).

Cell-based GPCR signaling assay

Stably transfected HEK 293 cells expressing Mth-B were plated in clear-bottom 96-well plates at ~25% confluency using Matrigel (BD Biosciences). Supernatant was removed by careful aspiration and each well was washed with 200 µl of buffer F [20 mM HEPES-KOH at pH 7.5, 0.1% (w/v) BSA, and 2.5 mM probenicid (dissolved first in 1/100 volume of 1 M NaOH) in Hanks' balanced salt solution without phenol red (HBSS,

Invitrogen)]. Fluo-4 (4 μM, dissolved first in 20 μL of 1:1 DMSO:10% Pluronic F-127, Molecular Probes) in buffer F with 1% BSA was added to each well (100 μl) and the plate was incubated at room temperature for 45 min, followed by incubation at 37 °C for 15 min. Wells were washed with 3 × 200 μL of buffer F while the plate was on ice. Buffer F (80 μl) was added to each well and the plate was incubated at 37 °C for 15 min prior to starting the experiment. Fluorescence measurements and automated sample delivery were performed on a robotic plate reader (Flexstation, Molecular Devices). Potential antagonists were added (20 μl) after the baseline readings followed by addition of the agonist peptide (50 μl) in reagent buffer (20 mM HEPES-KOH at pH 7.5 and 5% DMSO in HBSS). Continuous readings were made for ~5 min (7 reads per well, 2 s intervals, 494 nm excitation wavelength, 520 nm emission, and 515 nm cutoff filter). Data analysis and background subtraction were performed with Softmax Pro 4.7.1 (Molecular Devices). Sigmoidal fits were calculated using Origin 6.0 Professional (OriginLab).

References

1. West, A.P., Jr., Llamas, L.L., Snow, P.M., Benzer, S. & Bjorkman, P.J. Crystal structure of the ectodomain of Methuselah, a *Drosophila* G protein-coupled receptor associated with extended lifespan. *Proc. Natl. Acad. Sci. U.S.A.* **98**, 3744-3749 (2001).
2. Schatz, P.J. Use of peptide libraries to map the substrate specificity of a peptide-modifying enzyme: a 13 residue consensus peptide specifies biotinylation in *Escherichia coli*. *Bio-Technol.* **11**, 1138-1143 (1993).
3. Ja, W.W. & Roberts, R.W. *In vitro* selection of state-specific peptide modulators of G protein signaling using mRNA display. *Biochemistry* **43**, 9265-9275 (2004).
4. Otwinowski, Z. & Minor, W. Processing of x-ray diffraction data collected in oscillation mode. *Methods Enzymol.* **276**, 307-326 (1997).
5. Navaza, J. AMoRe: an automated package for molecular replacement. *Acta Crystallogr. A* **50**, 157-163 (1994).

6. Collaborative Computational Project, N. The CCP4 suite: programs for protein crystallography. *Acta Crystallogr. D* **50**, 760-763 (1994).
7. Brünger, A.T. et al. Crystallography & NMR system: A new software suite for macromolecular structure determination. *Acta Crystallogr. D* **54**, 905-921 (1998).

Supp. Table 1. Sequences of the selected peptides. Only the random region of the peptide library is shown. For peptides that appeared more than once, the frequency out of the total number of clones sequenced for that round is shown. Marked sequences (*) contain deletions or mutations that modify the constant C-terminal peptide (not shown). The sequence for R7-07 presumes that translation started at an alternate methionine codon in the random region, as the originally encoded methionine was followed by several stop codons. Related peptides that appeared in more than one selection round are color-coded.

	Clone	Peptide sequence		Frequency
Round 5	R5-01	NQKFSPERFTVWWLRASSALLRVPGLR		2/14
	R5-02	IQLVNMPRVGTLRRANMNMSPWRARCR	*	
	R5-03	RYVWYLRTKHRRSLRLRSACARGSSA	*	
	R5-04	HLFSWRDYPWHWVYRSLLARAPRP		3/14
	R5-05	SSLSPPWPASWSPSRPSAPRAAPSTPT	*	
	R5-07	APRAVWIQRAIQAMFRLASRQESKAFN		
	R5-08	KWLVLGRPVQWFVRTLMAMHQAGGSMI		
	S5-01	SNPKMPSLWLVLLSLHTRNEFPNSVSV		2/14
	S5-04	PKKWIQRHIRALRARTWSYFFLSRTR		
	S5-06	LPLEWFERSSSAAAAASWGRPPRRSG	*	
Round 7	R7-01	IVSWGSFPSSWLQRYYLAKRREADVTL		
	R7-02	VRIGYTSKPGGMNPGNSYTMSIIRMLI		
	R7-03	SSLSPPWPASWSPSRPSAPRAAPSTPT	*	
	R7-05	ELGQFQRLGLPYQWYLRTISYVTFRTA		
	R7-06	VLYPREWFFRAWKSYNASNAGLKDTPR	*	
	R7-07	RSPWARQFPEWDRMRNHMNPI	*	
	R7-08	IYSAYPVSWVARTCAATRARSAGARSA	*	
Round 8	R8-01	NVSWGSFPSSWLQRYYLAKRREADVTL		4/20
	R8-03	GDDMYRIREFLANYRPIWVMRSNLAQL		
	R8-04	VRIGYTSKPGGMNPGNSYTMSIIRMLI		7/20
	R8-07	LKYPDTWLARSLSVFYLRKSARQGKSV		
	R8-12	RLVWIVRSRHFGPRLRMALLGSDRKMW		
	R8-13	ELGQFQRLSLPYQWYLRTISYVSLRTA		
	R8-14	APRAVWIQRAIQAMFRLASRQESKAFN		
	R8-07b	STAGSRARSTSWGTRSPWTWPTPARTG	*	
	R8-08b	SSLSPPWPASWSPSRPSAPRAAPSTPT	*	2/20
	R8-09b	RYVWYLRTKHRRSLRLRSACARGSSA	*	

Supp. Table 2. Data collection and refinement statistics

Data collection	
Space group	$P4_2$
Cell dimensions	
a, *b*, *c* (Å)	94.23, 94.23, 173.83
Resolution (Å)	3.5 (3.62-3.5) *
R_{sym} or R_{merge}	0.155 (0.37)
$I / \sigma I$	7.5 (2.4)
Completeness (%)	95.3 (96.9)
Redundancy	3.7 (3.7)
Refinement	
Resolution (Å)	3.5
No. reflections	16870
R_{work} / R_{free}	0.374 / 0.408
No. atoms	
Protein	1529
Ligand/ion	0
Water	0
R.m.s. deviations	
Bond lengths (Å)	0.006
Bond angles (°)	1.35

One crystal was used in this structure determination. *Highest-resolution shell is shown in parentheses.

Supp. Fig. 1. Selected peptides recognize the full-length Mth receptor. (**a**) Fluorescence microscopy of CHO cells transiently transfected with a Mth-GFP fusion construct. Cells expressing Mth-GFP (left) were stained with 150 nM rhodamine-tagged R8-12 (right). Staining was not observed on cells incubated with a rhodamine-labeled, scrambled version of R8-12 or on control cells not expressing Mth. (**b**) Unstained cells, sorted by fluorescence-activated cell sorting, exhibited a range of Mth-GFP expression (left). Staining with rhodamine-R8-12 (right) revealed a direct correlation between the level of Mth-GFP expression (X-axis) and the degree of staining (Y-axis). The slight tailing at high GFP levels (left panel) is due to uncompensated crosstalk between the GFP and rhodamine channels.

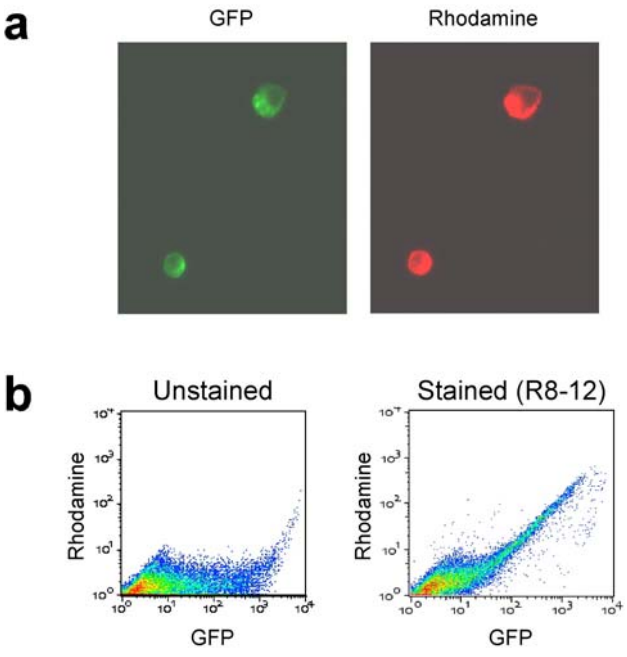

Supp. Fig. 2. Percentage of amino acid types at each position in (**a**) PxxWxxR (9 sequences) and (**b**) RxxWxxR (4 sequences) peptides. An Arg at the first position in the RWR motif is generally followed by two non-polar residues. Pro is followed by charged or polar amino acids, which may make up for any electrostatic contacts lost in the substitution of Pro for Arg. Residues 5 and 6 of the consensus motif are generally non-polar, while residue 8, immediately C-terminal to the RWR motif, is almost always polar, especially favoring Ser or Thr. There also seems to be a weak preference for Arg residues C-terminal to the RWR motif; Phe-Arg, Ala-Arg, and especially Leu-Arg pairs were often observed 5 to 7 residues downstream of the RWR motif (**Supp. Table 1**).

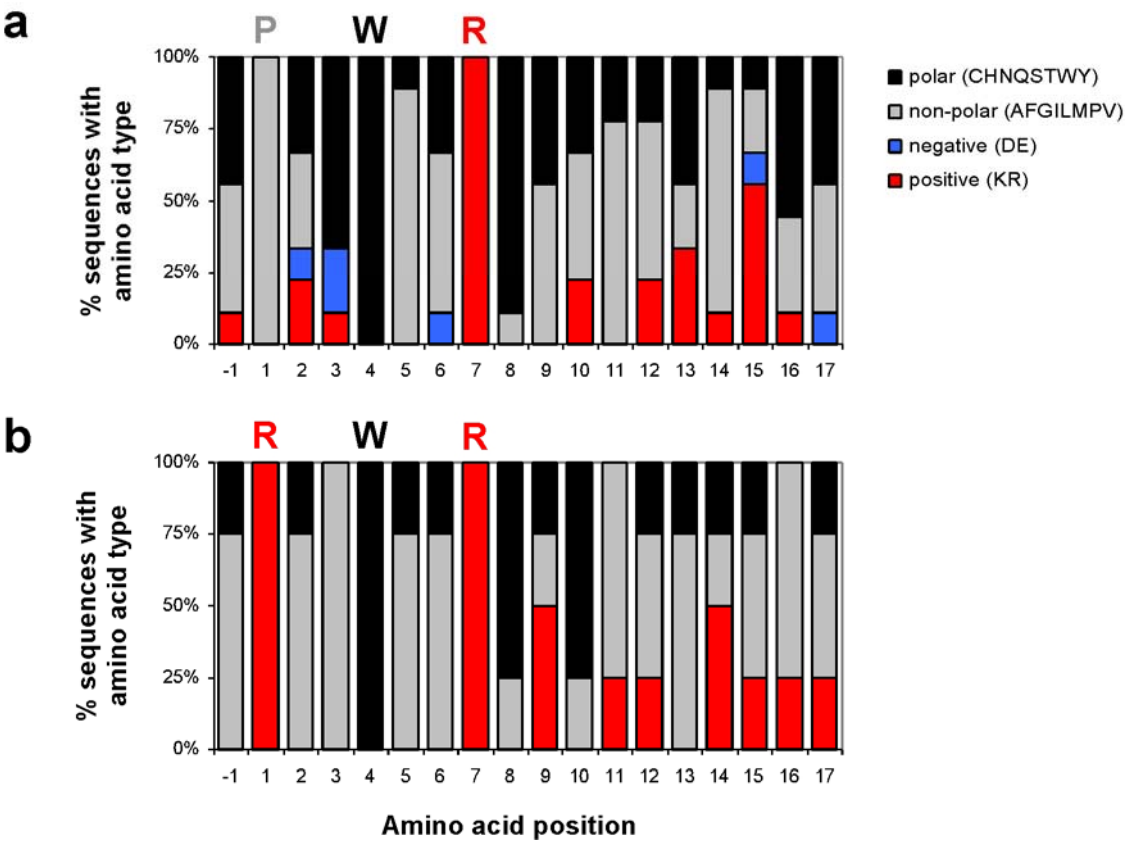

Supp. Fig. 3. Mth ligand binding site is not localized to Trp120. (**a**) Intrinsic tryptophan fluorescence of the Trp-less Mth W120S ectodomain, R8-12 peptide, and their complex upon excitation at 295 nm. The R8-12 peptide by itself exhibited maximum fluorescence at 351 nm, indicative of denatured proteins, suggesting that the peptide is unstructured in solution. A blue-shift of the maximum fluorescence wavelength (λ_{max}) to 343 nm and the increase in fluorescence upon binding to Mth W120S suggest that R8-12 Trp5 is at least partially buried in the complex and protected from solvent quenching. (**a**, inset) Fluorescence titration of 300 nM R8-12 peptide with Mth W120S (emission wavelength = 345 nm). The calculated K_D was 15 nM, consistent with results from the SPR studies on wild-type Mth. (**b**) Fluorescence spectra of wild-type Mth ectodomain with and without R8-04 peptide (which does not contain a Trp residue) upon excitation at 295 nm. The concentration of each component (3 μM) was ~10-fold greater than the K_D determined by SPR, suggesting that the lack of a fluorescence change was not due to inadequate complex formation. Our results indicate that Trp120 is not required for RWR motif peptide affinity and that the putative shared binding site for the selected peptides and the N-Stunted agonist is not likely to be near Trp120 in the Mth ectodomain.

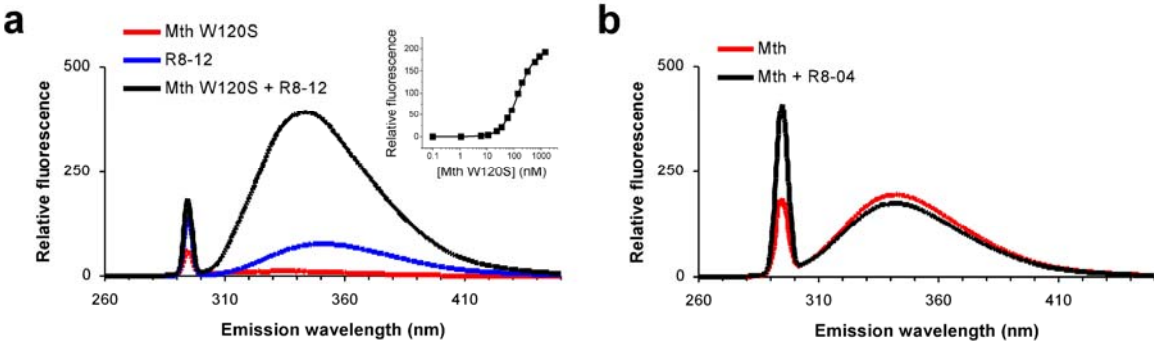

Supp. Fig. 4. Expression of the Mth antagonist R8-12 peptide extends fly lifespan. (**a**) Survival curves of male adult flies maintained at 29 °C for the UAS–R8-12 transgene insertion lines 11.1 and 41.2. These two lines, along with the 41.6 line shown in Fig. 4, are independent transformants. R8-12 expression extended mean adult lifespan by 40% and 31% in the 11.1 and 41.2 lines, respectively (average of two independent trials). The maximal adult lifespans were increased by 14% and 13%, respectively. (**b**) Survival curves of male adult flies comparing homozygous parental strains (w^{1118}, *da*-GAL4, and UAS–R8-12$^{41.6}$, in red) with the two non-peptide–expressing F1 heterozygous controls (*da*-GAL4 and UAS–R8-12$^{41.6}$, each crossed with w^{1118}, in black) at 29 °C. (**c**) Survival curves of male adult flies maintained at 25 °C for the UAS–R8-12 transgene insertion line 41.6. R8-12 expression extended the mean and maximal adult lifespans by 49% and 36%, respectively (average of two independent trials). Two independent experiments for each line are shown, and N = approximately 90 to 120 for each curve.

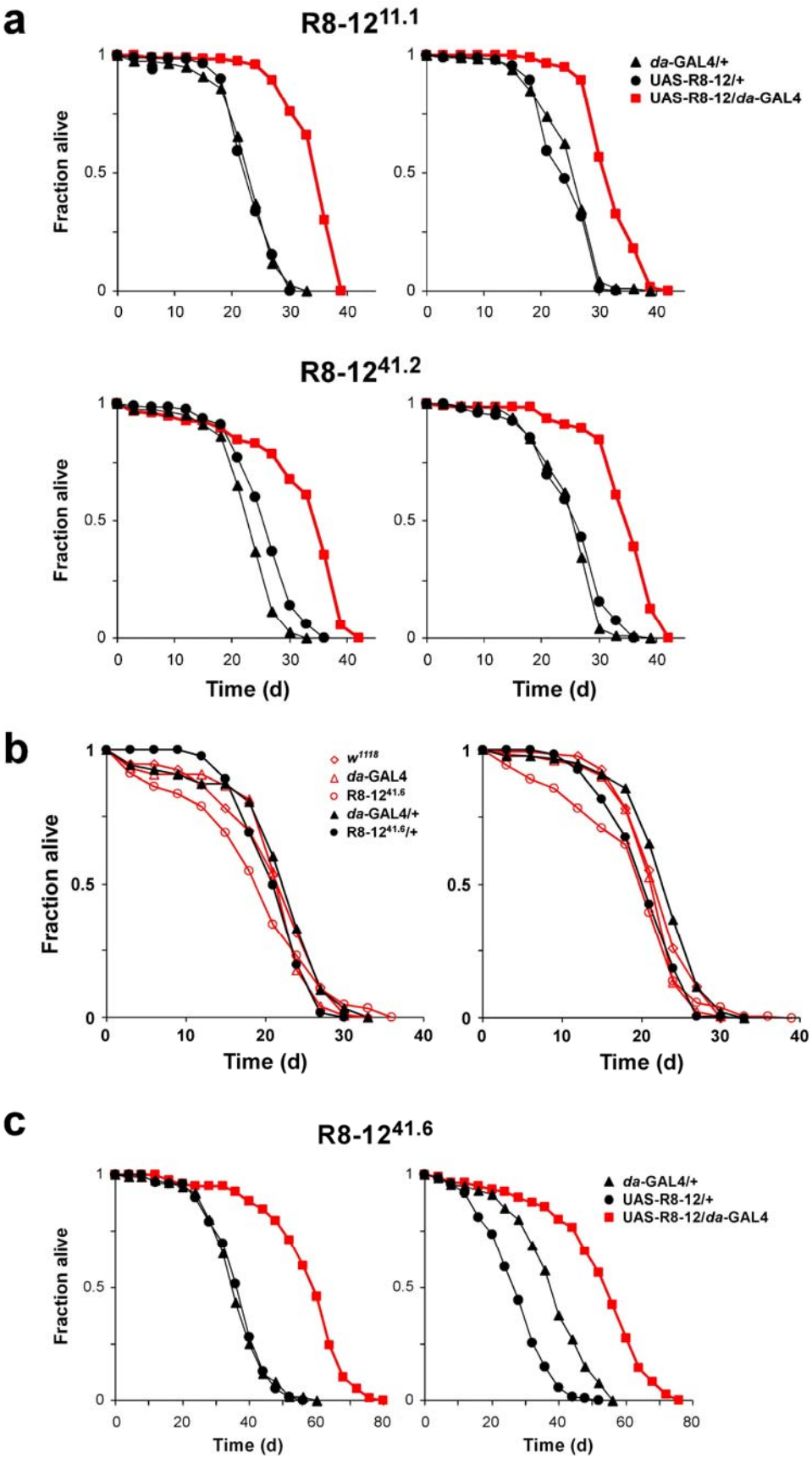
a
R8-12^11.1
R8-12^41.2
Fraction alive
Time (d)
da-GAL4/+
UAS-R8-12/+
UAS-R8-12/da-GAL4
b
w^1118
da-GAL4
R8-12^41.6
da-GAL4/+
R8-12^41.6/+
c
R8-12^41.6

Supp. Fig. 5. Binding interaction of R8-04 peptide with immobilized Mth ectodomain, measured by SPR. The indicated concentrations of R8-04 peptide were injected (45 μl at 0 s, at a 45 ml min^{-1} flow rate) across ~500 response units (RU) of immobilized Mth-biotin. Raw data were processed with Scrubber and fit with CLAMP using a 1:1 bimolecular interaction model[8]. The global kinetic fits (black) are overlaid on the original sensorgrams (gray). The derived kinetic parameters are shown in Table 1. Sensorgrams have been double-referenced from response curves generated by an appropriate negative control flow cell and averaged buffer blank injections. Three buffer blank injections are shown (0 nM).